STUDY OF THE CRYSTALLIZATION FIELDS OF NICKEL(II) SELENITES IN THE SYSTEM NiSeO₃–SeO₂–H₂O

L. T. Vlaev[*], Svetlana D. Genieva and Velyana G. Georgieva

Department Physical Chemistry, Assen Zlatarov University, 8010 Bourgas, Bulgaria

The solubility of $NiSeO_3$–SeO_2–H_2O system in the temperature region 298–573 K was studied. The compounds of the three-component system were identified by the Schreinemakers' method. The phase diagram of nickel(II) selenites was drawn and the crystallization fields for the different phases were determined. Depending on the conditions for hydrothermal synthesis, $NiSeO_3 \cdot 2H_2O$, α-$NiSeO_3 \cdot 1/3H_2O$, β-$NiSeO_3 \cdot 1/3H_2O$, $NiSeO_3$ and $NiSe_2O_5$ were obtained. The different phases were proved and characterized by chemical, powder X-ray diffraction and thermal analyses as well as IR spectroscopy.

Introduction

Various nickel(II) selenites have been reported in the literature [1–18]. It is known $NiSeO_3 \cdot 4H_2O$ [15], $NiSeO_3 \cdot 2H_2O$ [1–4, 6–10, 12, 17], $NiSeO_3 \cdot H_2O$ [3, 17], $NiSeO_3 \cdot 1/3H_2O$ [13, 14, 17], $NiSeO_3$ [3, 11, 17], $Ni(HSeO_3)_2 \cdot 4H_2O$ [16], $Ni(HSeO_3)_2 \cdot 2H_2O$ [12] and $NiSe_2O_5 \cdot 3H_2O$ [5]. Only $NiSeO_3 \cdot 2H_2O$ can be found in the natural form of a mineral – ahlfeldite [19]. Under common conditions, $NiSeO_3 \cdot 2H_2O$ crystallizes from aqueous solutions [1–4, 6–10, 12, 17]. $NiSeO_3 \cdot 2H_2O$ is isomorphous with other hydrated divalent selenites $MSeO_3 \cdot 2H_2O$ (*M*=Mg, Mn, Co, Cu, Zn) [6, 18]. Its thermal dehydration, however, does not produce lower crystallohydrates as separate phases [7, 9, 10]. They can be obtained by hydrothermal treatment at temperatures above 373 K [13, 18] or by employing other special conditions or reagents [2, 18]. Heated to temperatures within 523–573 K, $NiSeO_3 \cdot 2H_2O$ dehydrates to transform into $NiSeO_3$ [7, 10].

The lack of systematic approach in most of the studies cited does not allow to determine clearly the types and number of the different solid phases which are in equilibrium with the liquid phase at various temperatures, as well as the boundaries of the crystallization fields of the known nickel(II) selenites in the system $NiSeO_3$–SeO_2–H_2O. In this respect, useful information can be obtained from the dissolution isotherms of the system at different temperatures and the values of the parameters characterizing the none variant (peritonic) points.

The aim of the present work is to study the crystallization fields of nickel(II) selenites in the system $NiSeO_3$–SeO_2–H_2O in the temperature interval 298–573 K and characterize the phases observed.

Experimental

The initial substance used was $NiSeO_3 \cdot 2H_2O$. It was prepared by precipitating a 0.2 equiv L^{-1} aqueous solution of nickel(II) chloride hexahydrate puriss. (Merck) with a 0.2 equiv L^{-1} aqueous solution of sodium selenite pentahydrate puriss. (Fluka) at 298 K. The solutions with volumes of 1 L were slowly mixed (5 cm^3 min^{-1}) under continuous stirring with blade mixer. The precipitate obtained was 'aged' in the initial solution at room temperature for a week. The crystalline substance formed was collected on a G4 frit, rinsed vigorously with deionized distilled water and dried in air at ambient temperature for another week. The isolated compound was light-green crystalline powder, which was stable in air at laboratory temperature. The results from the chemical and powder X-ray analyses showed the compound had net formula $NiSeO_3 \cdot 2H_2O$. Thus, the $NiSeO_3 \cdot 2H_2O$ obtained was used as initial substance for the study of the solubility in the $NiSeO_3$–SeO_2–H_2O system at different temperatures. Teflon-lined steel vessels with volume 20 cm^3 were used for the experiment [20]. In these vessels, 1 g $NiSeO_3 \cdot 2H_2O$ and 15 cm^3 aqueous solution of SeO_2 puriss. (Merck) with concentrations varying from 0 to 70 mass% SeO_2 in 5% steps were placed. The time required for equilibration of the individual samples was from 2 months (at 298 K) to 20 days (at 573 K). The temperatures of the hydrothermal synthesis ranged from 298 to 573 K in 50 K steps. At the end of experiment time, the vessels were cooled and opened and the precipitate was filtered through porous glass filter. Both precipitate and filtrate were analysed to determine the contents of nickel(II) and selenium(IV). Selenium(IV) was determined iodometrically by Kotarski method [21]. Nickel(II) was titrated complexometrically using

---

[*]   Author for correspondence: vlaev@btu.bg

xylenol orange as an indicator [22]. The Schreine-maker's method was used to study the solubility in the $NiSeO_3$–SeO_2–H_2O system. The solubility diagram was drawn according to Gibbs–Roozeboom method [23, 24].

Powder X-ray patterns were taken on a wide angle X-ray diffractometer with a goniometer URD-6 (Germany), using cells with a diameter of 12 mm, CoK_α radiation (λ=1.78892 Å) and an iron filter for β-emission. The lattice parameters were derived from 150–165 accurately measured reflections in the range $3 \leq 2\theta \leq 60°$. The structures were solved by Patterson or direct methods and refined with the least squares method.

The thermal analyses of the samples was performed on a Paulik–Paulik–Erdey apparatus (MOM, Hungary) by heating to 1073 K at heating rate 10 K min^{-1} in a flow of nitrogen at a rate of 20 cm^3 min^{-1}. The samples (100 mg) were vigorously ground in agate vibration mortar. The standard used was α-Al_2O_3 heated to 1373 K. The curves were registered with resolutions 1/5 for DTA, 1/15 for DTG and 1 mg for TG.

The IR absorption spectra were taken on a spectrophotometer Specord-75 (Carl Zeiss, Jena, Germany) over the region from 400 to 4000 cm^{-1} (resolution 1 cm^{-1}). The experiments were carried out at room temperature using KBr pellets with concentration of the substance studied 0.3 mass%.

Results and discussion

The Schreinemakers' method was used to study solubility in the $NiSeO_3$–SeO_2–H_2O system. The solubility diagrams obtained at 423 and 573 K, constructed by the Gibbs–Roozeboom method, are presented in Fig. 1.

Schreinemakers' data show (Fig. 1a) that two solid phases crystallize in the system at 423 K – $NiSeO_3 \cdot 2H_2O$ and $NiSe_2O_5$. The peritonic point between $NiSeO_3 \cdot 2H_2O$ and $NiSe_2O_5$ is at 4.3 mass% $NiSeO_3$, 26.5 mass% SeO_2 and 69.2 mass% H_2O. At 573 K (Fig. 1b) Schreinemakers' data show that three solid phases crystallize in the system – $NiSeO_3 \cdot 1/3H_2O$, $NiSeO_3$ and $NiSe_2O_5$. The $NiSeO_3 \cdot 1/3H_2O$ resulting from the hydrothermal synthesis lost its crystallization water at temperature above 573 K and SeO_2 content higher than 22 mass% to transform into anhydrous $NiSeO_3$. The peritonic point P_1 corresponds to 2.9 mass% $NiSeO_3$, 17.4 mass% SeO_2 and 79.7 mass% H_2O. At SeO_2 concentration higher than 45 mass%, the anhydrous nickel selenite transforms into $NiSe_2O_5$. The peritonic point P_2 corresponds to 4.7 mass% $NiSeO_3$, 36.5 mass% SeO_2 and 58.8 mass% H_2O.

The results obtained from the experiments carried out showed that the following solid phases
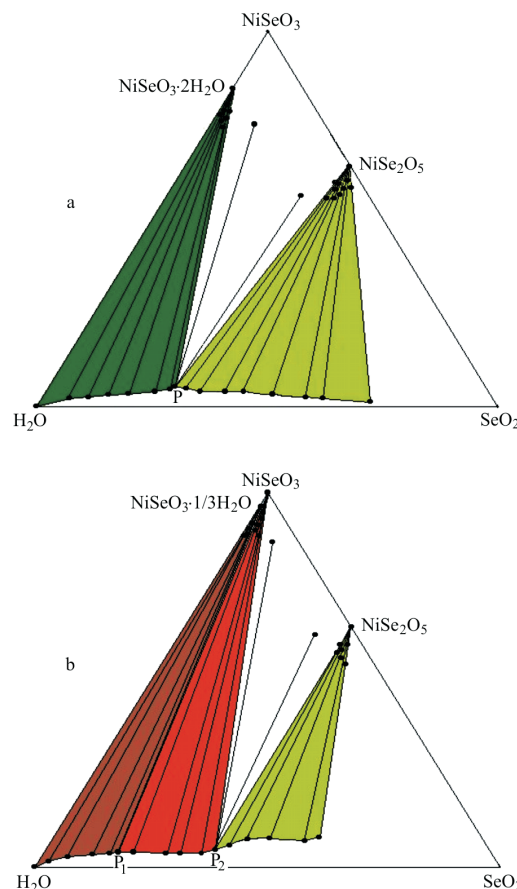

Fig. 1 Solubility isotherms of the system $NiSeO_3$–SeO_2–H_2O at: a – 423 and b – 573 K

formed in the system $NiSeO_3$–SeO_2–H_2O which was in equilibrium with the liquid phase (containing from 0 to 70 mass% SeO_2) within the temperature interval 298–573 K: $NiSeO_3 \cdot 2H_2O$ ($NiO \cdot SeO_2 \cdot 2H_2O$), $NiSeO_3 \cdot 1/3H_2O$ ($NiO \cdot SeO_2 \cdot 1/3H_2O$), $NiSeO_3$ ($NiO \cdot SeO_2$) and $NiSe_2O_5$ ($NiO \cdot 2SeO_2$). The individual phases were distinguishable by colour and crystalline habitus: $NiSeO_3 \cdot 2H_2O$ – light-green crystalline powder; $NiSeO_3 \cdot 1/3H_2O$ – citron-yellow, fine crystalline; $CoSeO_3$ – yellow-brown well crystallized and $NiSe_2O_5$ – light yellow, fine powder. The samples obtained were identified by the chemical, X-ray diffraction and IR spectroscopy analyses.

The interplanar distances and the relative intensities of the peaks are given in Table 1.

According to literary data [5, 18], $NiSeO_3 \cdot 2H_2O$ adopted a structure similar to Cu, Mg, Zn, Mn and Co selenite dihydrates. The structure of $NiSeO_3$ was closely related to that of $CoSeO_3 \cdot 1/3H_2O$ [4, 14] and the isotypic compound $CoSeO_3 \cdot 1/3H_2O$ [6, 14]. $NiSe_2O_5$ was found to be isomorphous with $ZnSe_2O_5$, $CoSe_2O_5$ and $MnSe_2O_5$ [6, 18]. Table 2 summarizes the parameters characterizing the crystalline lattices of the selenites studied.

Table 1 The interplanar distance (nm) and the relative intensity (%) of the peaks

NiSeO₃·2H₂O			α-NiSeO₃·1/3H₂O			β-NiSeO₃·1/3H₂O			NiSeO₃			NiSe₂O₅		
d/nm	I	h k l	d/nm	I	h k l	d/nm	I	h k l	d/nm	I	h k l	d/nm	I	h k l
0.56845	100	0 1 1	0.72718	11	0 1 −1	0.67885	6	1 0 0	0.81008	25	1 1 2	0.56807	2	0 1 1
0.52146	19	1 0 1	0.62471	70	0 1 0	0.58315	25	0 1 1	0.72229	88	2 0 0	0.41494	3	1 1 1
0.44826	11	1 1 1	0.39815	7	1 −1 −1	0.36291	12	0 0 2	0.59152	13	1 1 −2	0.33957	100	0 0 2
0.44125	26	1 1 −1	0.36361	100	2 0 0	0.36064	19	0 2 1	0.43332	10	3 1 0	0.30797	45	0 3 1
0.32056	21	1 1 2	0.34067	3	2 −2 1	0.31540	11	2 0 2	0.40931	28	2 2 0	0.28499	13	1 1 2
0.29678	73	2 1 0	0.29224	6	2 0 −2	0.29338	18	2 2 0	0.37982	11	3 1 1	0.28404	58	0 2 2
0.27087	36	1 2 2	0.27438	67	0 1 −3	0.28435	100	2 −1 1	0.36811	27	2 0 −4	0.27469	20	1 3 1
0.25171	18	2 2 1	0.26650	9	2 1 0	0.26617	10	2 1 −1	0.36114	45	4 0 0	0.26788	16	2 1 1
0.24413	16	1 0 3	0.25072	27	2 −1 −2	0.24488	32	0 3 0	0.34300	13	2 2 −3	0.25915	32	0 4 0
0.23519	43	1 1 3	0.24925	25	1 2 0	0.23552	12	3 1 0	0.32281	19	1 3 0	0.23837	5	1 4 0
0.22291	11	1 3 2	0.24393	16	0 3 −1	0.22775	6	1 −2 −2	0.30434	21	4 2 −1	0.22116	24	0 1 3
0.21933	33	0 4 0	0.21734	4	2 1 1	0.21629	8	1 3 −1	0.29760	19	1 1 4	0.19829	8	0 5 1
0.21186	11	2 3 1	0.20744	6	2 −4 2	0.20106	4	2 −3 1	0.29224	45	5 1 −1	0.19510	9	1 4 2
0.20218	6	1 4 1	0.20035	7	4 −1 0	0.19438	7	0 3 3	0.28392	60	0 2 4	0.18937	11	2 3 2
0.19495	11	3 0 −1	0.19483	3	3 0 −3	0.19385	3	2 0 4	0.27742	100	5 1 0	0.18934	10	2 4 1
0.18741	4	1 3 3	0.18748	3	1 −3 −1	0.18809	4	0 3 3	0.27445	23	3 1 3	0.18175	8	3 2 1
0.17830	5	2 3 −2	0.18280	14	2 3 −3	0.18665	4	1 −2 −3	0.24486	55	0 4 1	0.17277	10	0 6 0
0.17169	27	0 2 4	0.17567	17	3 2 −1	0.18110	8	3 0 4	0.24036	73	3 3 −4	0.16989	32	1 5 2
0.16905	8	1 5 0	0.17135	14	2 3 −1	0.17896	6	4 3 −2	0.24007	62	4 2 −5	0.16978	31	0 0 4
0.16784	10	2 4 2	0.16758	16	1 2 −3	0.17333	20	2 −3 1	0.20414	29	1 3 5	0.16489	7	3 2 2
0.16285	8	3 3 2	0.16551	31	4 −1 2	0.16862	5	2 4 −2	0.18481	53	1 5 −3	0.16152	13	1 1 4
0.16003	3	1 2 −4	0.16531	20	4 −5 −3	0.16439	9	0 4 3	0.18418	39	4 4 −5	0.16135	11	0 2 4
0.15879	9	0 5 2	0.15839	34	5 −3 1	0.16013	4	3 5 4	0.17997	10	6 4 −2	0.16069	2	2 3 3
0.15658	3	4 1 1	0.15816	21	4 2 2	0.15630	8	5 1 2	0.17175	28	8 2 0	0.15957	11	3 4 0
0.15486	7	2 3 −3	0.15522	4	3 −2 −3	0.15615	6	0 −3 1	0.15662	5	2 6 −3	0.15534	2	3 4 1

Table 2 Crystallographic data for nickel(II) selenites

Parameter	$NiSeO_3\cdot2H_2O$	α-$NiSeO_3\cdot1/3H_2O$	β-$NiSeO_3\cdot1/3H_2O$	$NiSeO_3$	$NiSe_2O_5$
colour	light-green	citron-yellow	citron-yellow	yellow-brown	light-yellow
space group	$P2_1/n$	P-1	P-1	C2/c	Pnab
a/nm	0.63782	0.81383	0.80222	1.54915	0.60754
b/nm	0.87734	0.84034	0.82133	0.99355	1.03662
c/nm	0.75467	0.85724	0.84364	1.48416	0.67913
α/°	–	123.713	68.654	–	–
β/°	81.451	90.174	61.782	111.173	–
γ/°	–	111.823	66.363	–	–
Z	4	2	2	32	4
V/nm^3	0.41761	0.43583	0.43811	0.213015	0.42771
d_R/g cm^{-3}	3.524	1.429	1.422	4.630	4.605

The comparison of the parameters measured was in very good accordance with data obtained from other authors [2, 4, 5, 7, 12, 13, 18]. It should be noted that two separate isomorphous phases (α and β) were observed for both $NiSeO_3\cdot1/3H_2O$ and $CoSeO_3\cdot1/3H_2O$ and they had different parameters of the crystalline lattice. Their IR spectra, however, were identical.

On the basis of the solubility diagrams of $NiSeO_3$–SeO_2–H_2O system at different temperatures and the compositions at the peritonic points in the Gibbs–Roozeboom diagrams, the polythermal diagram of the system studied was drawn (Fig. 2).

As can be seen from the figure, five different by area crystallization fields and three nonevariant points each with three solid phases in equilibrium can be identified. If the composition of the different selenites is described by the general formula $NiO\cdot nSeO_2\cdot mH_2O$, then Fig. 2 shows that phases with small m became stable with the increase of temperature while the phases with small n were more stable with decreased SeO_2 concentration. The boundaries between the crystallization fields with different values of m, however, were

not horizontal and those for different n were not vertical. Each boundary had its slope (negative or positive). Similar pattern was observed for the crystallization fields of iron(III) selenites [25]. At SeO_2 concentrations lower than 30 mass%, the increase of temperature lead to formation of thermodynamically stable selenites phases with lower values of m: $NiSeO_3\cdot2H_2O\rightarrow$ $NiSeO_3\cdot1/3H_2O\rightarrow NiSeO_3$. Besides, the slope of the boundary between these two fields was negative ($dT/dx<0$). It means that, with the increase of SeO_2 concentration, the equilibrium shifts in the same direction in which it shifts with the increase of temperature, i.e. SeO_2 exerts dehydrating effect and the values of m in the general formula decrease from 2 to 0 (fields I, II and III) and from 2 to 0 (fields I, V and VI). Similar considerations can be applied to the values of n at T=const. and varying SeO_2 concentration. In all the cases studied, the equilibrium shifted to compounds with lower values of n (from 2 to 1, fields V and I and fields V and IV) with the decrease of SeO_2 concentration in the solution, i.e. hydrolyzation was facilitated. The slopes of the curves separating fields 1, II, III and IV were negative because the increase of temperature and SeO_2 concentration in the solution eased selenites dehydration. The results obtained clearly showed that the hydrothermal treatment of $NiSeO_3\cdot2H_2O$ does not give $NiSeO_3\cdot H_2O$ and $NiSe_2O_5\cdot3H_2O$ in the temperature and concentration intervals studied. As it has been reported earlier [10, 18], monohydrate was not observed as intermediate product by the dehydration of the dihydrate and, likewise, $NiSeO_3\cdot1/3H_2O$ was not observed by the dehydration of $NiSeO_3\cdot H_2O$. According to the same authors, the reason for this lack of continuity was the incompatibility of the texture of these crystallohydrates. Figure 3 shows TG, DTA and DTG curves of thermal dehydration of $NiSeO_3\cdot2H_2O$ and decomposition of $NiSeO_3$.
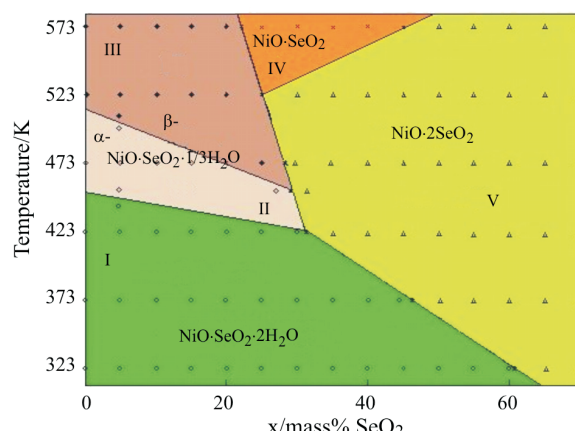

Fig. 2 Crystallization field of selenites in $NiSeO_3$–SeO_2–H_2O system
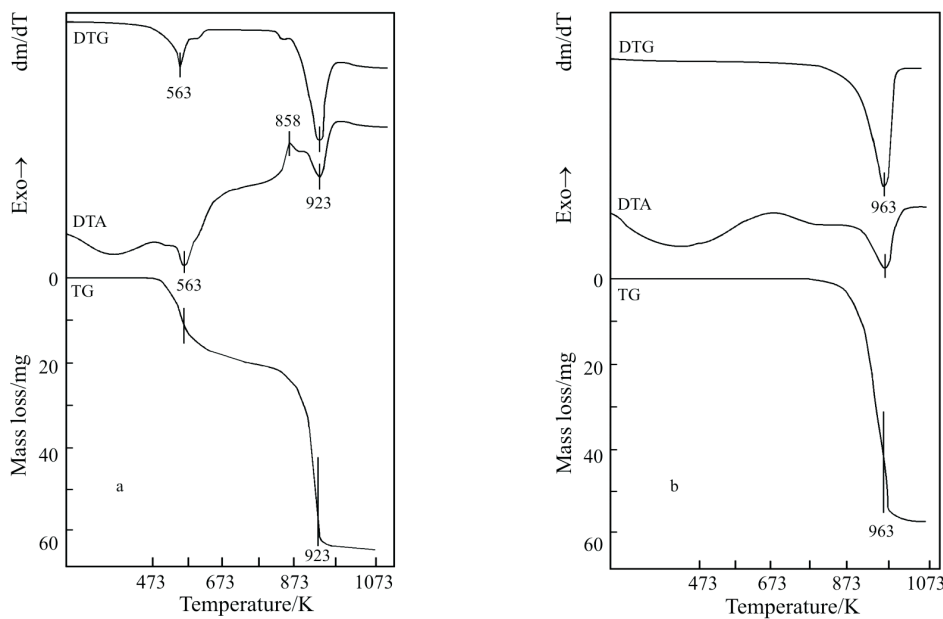
Fig. 3 TG, DTG and DTA curves of dehydration and decomposition of: a – $NiSeO_3 \cdot 2H_2O$ and b – $NiSeO_3$

As can be seen from the Fig. 3a the dehydration of $NiSeO_3 \cdot 2H_2O$ was a one-stage process giving $NiSeO_3$ (mass loss 16.2 mass%) and the product obtained was found to be X-ray amorphous. Intermediate products of the dehydration like $NiSeO_3 \cdot H_2O$ and $NiSeO_3 \cdot 1/3H_2O$ were not registered. The highest dehydration rate was measured at 563 K. An exo-effect was observed at 858 K and attributed to the crystallization of the amorphous phase [10]. Data from both X-ray and chemical analyses showed that the product corresponds to the formula $NiSeO_3$. At temperatures above 873 K it started to decompose by releasing SeO_2 and formation of NiO. The decomposition was accomplished at about 973 K (mass loss 49.9 mass%) and the highest decomposition rate was observed at 923 K. Figure 3b shows TG, DTA and DTG curves of decomposition of $NiSeO_3$ prepared under hydrothermal regime of precipitation.

It can be seen that the decomposition proceeded at maximum rate at temperature of 963 K, which is by 40 K higher than the decomposition temperature of $NiSeO_3 \cdot 2H_2O$. It can be explained with the greater stability of the crystal lattice of $NiSeO_3$ obtained by hydrothermal synthesis compared to that of the same product obtained in situ by dehydration of $NiSeO_3 \cdot 2H_2O$. Based on the method of Coats and Redfern [26, 27] for the kinetics of topochemical reactions under non-isothermal conditions of heating, the values of the activation energy E, frequency factor A in Arrhenius equation, changes of entropy $\Delta S^{\neq}$, Gibbs free energy $\Delta G^{\neq}$ and enthalpy $\Delta H^{\neq}$ of the processes of dehydration and decomposition of $NiSeO_3 \cdot 2H_2O$ and decomposition of $NiSeO_3$ were calculated. These values are presented in Table 3.

As can be seen from Table 3, the dehydration of $NiSeO_3 \cdot 2H_2O$ is characterized by twice lower value

Table 3 Kinetic parameters of non-isothermal dehydration and decomposition of $NiSeO_3 \cdot 2H_2O$ and $NiSeO_3$

Parameter	$NiSeO_3 \cdot 2H_2O$		$NiSeO_3$
	dehydration	decomposition	decomposition
R^2	0.9914	0.9981	0.9982
n	2.0	1.0	1.0
E_a/kJ mol^{-1}	93.6	189.2	213.2
A/min^{-1}	$2.53 \cdot 10^8$	$9.63 \cdot 10^{12}$	$6 \cdot 10^{13}$
$-\Delta S^{\neq}$/J K^{-1} mol^{-1}	131.5	48.1	32.2
$\Delta H^{\neq}$/kJ mol^{-1}	89.0	181.5	205.1
$\Delta G^{\neq}$/kJ mol^{-1}	161.7	225.9	236.2
T_p/K	553	923	963

The values of $\Delta S^{\neq}$, $\Delta H^{\neq}$ and $\Delta G^{\neq}$ are calculated at corresponding T_p temperature.
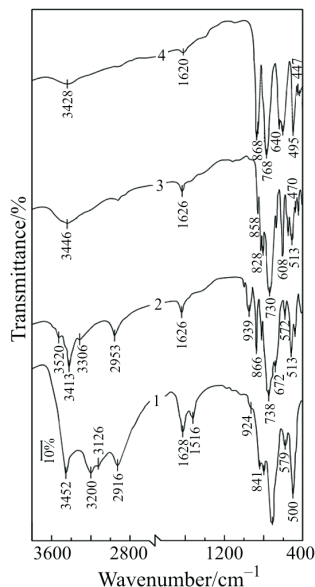
Fig. 4 Infrared absorption spectra of nickel(II) selenites at 298 K: 1 – NiSeO$_3$·2H$_2$O, 2 – NiSeO$_3$·1/3H$_2$O, 3 – NiSeO$_3$ and 4 – NiSe$_2$O$_5$

of the activation energy compared to that of decomposition. Besides, the dehydration is described by kinetic equation of second order (n=2) while decomposition – by equation of first order (n=1). In all the cases studied, however, the change of entropy $\Delta S^{\neq}$ for the formation of the activated complex was negative, which means that the complex has higher degree of arrangement compared to the initial reagent. The higher absolute values of $\Delta S^{\neq}$ for the dehydration compared to decomposition showed that the former process was accompanied by bigger rearrangement of NiSeO$_3$·2H$_2$O structure. The higher values of the activation energy of decomposition of NiSeO$_3$ obtained hydrothermally compared to the decomposition of NiSeO$_3$·2H$_2$O confirmed the higher thermal stability of the former product.

The different nickel(II) selenites obtained were studied by IR spectroscopy and the absorption spectra are presented in Fig. 4. The bands observed were interpreted according to the works of Simon [28, 29] and Cody [30, 31] for selenous acid and other authors, studying IR spectra of nickel(II) selenites [12, 15, 16] or another selenites [16, 32–34].

Figure 4 showed that IR spectra of the selenites studied had some common and some specific bands. For instance, four absorption bands were registered in the high frequency region of NiSeO$_3$·2H$_2$O spectrum, which were attributed to stretching vibrations of O–H from H$_2$O molecules. In the interval 1500–1700 cm^{-1} two absorption bands were observed due to the bending vibrations of H$_2$O molecules. The reason for this is that the two water molecules in the dihydrate are structurally unequal according to the following scheme [35]:
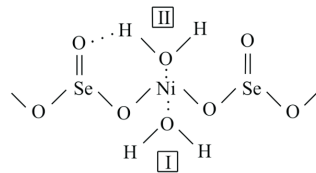
In the environment of the octahedral Ni^{2+} cation, one of the water molecules is at a distance equal to the sum of the covalent radii of the metal and oxygen and at almost equal distances from the oxygen atoms of the selenite group. This molecule (denoted as H$_2$O–I) is loaded almost symmetrically, therefore the difference in the frequencies of its asymmetric ν_{as} and symmetric ν_a vibrations is almost constant with a value of 100–110 cm^{-1} [32, 36]. Hence, the band at 3200 cm^{-1} can be attributed to $\nu_{as(O-H)(H_2O)}$ and the band at 3126 cm^{-1} – to $\nu_{s(O-H)(H_2O-I)}$. The second water molecule is at higher distance from Ni^{2+} ion but at a relatively small distance from Se=O (HOH...OSe<~2.7 Å), forming a strong enough hydrogen bond. The bond of the second hydrogen atom with the oxygen atom in the H$_2$O molecule remains almost the same as in a free water molecule. Since in such cases of asymmetric loading of the (H$_2$O–II) molecule the difference between the stretching vibrations could be as much as 500–600 cm^{-1} [36], then the vibrations along both O–H bonds in this molecule can be regarded as independent. Therefore, the band with the highest frequency at 3452 cm^{-1} can be attributed to $\nu_{free(OH)}$ of the relatively free OH group in (H$_2$O–II) while that at 2916 cm^{-1} – $\nu_{bond(OH)}$ of the OH group bonded by hydrogen bond in the same water molecule. Consequently, the band at 1516 cm^{-1} is probably due to the bending vibrations $\delta_{as(H_2O-I)}$ and the band at 1628 cm^{-1} – to $\delta_{as(H_2O-II)}$.

All these considerations were sustained by the fact that only one absorption band at 1626 cm^{-1} was observed for NiSeO$_3$·1/3H$_2$O, representing the bending vibrations of (H$_2$O–II) molecules, thus confirming that in this case the water molecules were structurally equal. Two clearly distinguishable bands at 3413 and 2959 cm^{-1} were registered in the high frequency region of the same spectrum. Since the difference between them was quite big (~400 cm^{-1}), they can be attributed to stretching vibrations of $\nu_{free(OH)}$ from (H$_2$O–II). For NiSeO$_3$, however, no absorption bands were observed from 1500 to 1300 cm^{-1} except for the low intensity broad bands at 1626 and 3446 cm^{-1} probably due to small quantities of physically adsorbed water on sample surface.

A number of bands were registered in the region 900–400 cm^{-1} and their number increased from NiSeO$_3$·2H$_2$O to NiSeO$_3$, i.e. as dehydration proceeds, the characteristic bands were more distinctly measured and the IR spectrum had more details. Four

Table 4 Infrared absorption spectra of $NiSeO_3 \cdot 2H_2O$ and $NiSeO_3 \cdot H_2O \cdot D_2O$

$NiSeO_3 \cdot 2H_2O$ ν/cm^{-1}	$NiSeO_3 \cdot H_2O \cdot D_2O$ ν/cm^{-1}	$\dfrac{\nu_{NiSeO_3 \cdot 2H_2O}}{\nu_{NiSeO_3 \cdot H_2O \cdot D_2O}}$	Band assignment
500 vs	493 s	1.014	$\delta_{SeO_3^{2-}}$
579 w	589 w	0.983	ν_{Ni-O}
700 vs	716 vs	0.978	$\nu_{as(SeO_3^{2-})}$
800 s	816 s	0.980	$\nu_{s(SeO_3^{2-})}$
841 s	854 w	0.985	$\nu_{s(SeO_3^{2-})}$
924 sh			ρ_{H_2O}
	1136 w	1.335	$\delta_{(OD)(D_2O)}$
	1200 w	1.357	$\delta_{(OD)(D_2O)}$
1516 m	1540 sh	0.984	$\delta_{(OH)(H_2O)}$
1628 s	1626 s	1.001	$\delta_{(OH)(H_2O)}$
	2213 s	1.318	$\nu_{(OD)(D_2O)}$
	2391 s	1.338	$\nu_{(OD)(D_2O)}$
	2550 s	1.354	$\nu_{(OD)(D_2O)}$
2916 s	2924 s	1.997	$\nu_{(OH)(H_2O)}$
3126 sh	3118 sh	1.003	$\nu_{(OH)(H_2O)}$
3200 s	3200 s	1.000	$\nu_{(OH)(H_2O)}$
3452 vs	3450 vs	1.001	$\nu_{(OH)(H_2O)}$

vs – very strong, s – strong, m – medium, w – weak, b – broad, sh – shoulder, ν_s – symmetric stretching, ν_{as} – antisymmetric stretching, δ – bending and ρ – rocking

types of characteristic bands were found: ν_{Se-O} in SeO_3^{2-} anion, ρ_{H_2O}, ν_{Co-O} and δ_{O-Se-O}. These absorption bands were observed in the IR spectra of the other selenites; they were analyzed by other authors [32, 36, 37].

The spectrum of $NiSe_2O_5$ (Fig. 4, spectrum 4) showed two low intensity and wide absorption bands at 3428 and 1620 cm^{-1}. They were due to the stretching and bending vibrations, respectively, of small amounts of physically adsorbed water on sample surface. Taking into account the composition and specific features of the thermal decomposition of the diselenites, $NiSe_2O_5$ can be regarded as a product of attachment – co-ordination bonding of a molecule SeO_2 to $NiSeO_3$. Therefore, the IR spectrum showed both absorption bands for the almost free SeO_2 [38, 39] and ions [34–39]. The large number of bands present in the interval 850–400 cm^{-1} are usually connected with the vibration structure of the diselenite anion $[O_2Se-O-SeO_2]$. The spectrum is considered to summarize the vibrations of (SeO_2)-groups and (Se–O–Se) bridges [34–39]. According to the authors who have studied various selenites, the bands in the interval 900–860 cm^{-1} are due to $\nu_{as(SeO_2)}$; 840–780 cm^{-1} – to $\nu_{s(SeO_2)}$; 600–560 cm^{-1} – $\nu_{as(Se-O-Se)}$; 530–475 cm^{-1} – $\nu_{s(Se-O-Se)}$; 410–330 cm^{-1} – $\delta_{(SeO_2)}$ and those from 300 to 250 cm^{-1} – to $\delta_{Se-O-Se}$.

The IR spectra of the samples obtained after treatment with D_2O confirmed the different thermal stability of the crystallization water (H2O–I) and (H2O–II) in $NiSeO_3 \cdot 2H_2O$ (Fig. 5).

The treatment of $NiSeO_3 \cdot 2H_2O$ with D_2O for 10 days followed by drying at 373 K did not lead to changes in the IR spectrum. It means that the H2O

molecules in the crystallohydrate were strongly bonded and were not exchanged with D_2O under these conditions. According to data from thermal and X-ray analyses, the heating of $NiSeO_3 \cdot 2H_2O$ to 473 K results in its partial dehydration and amorphization (spectrum 2). The five consecutive treatments of this sample with D_2O in autoclave at 473 K followed by drying at 373 K gave substantial changes in the IR spectrum (spectrum 3). Two new groups of absorption bands were registered at 1136, 1200 cm^{-1} and 2213, 2391, 2550 cm^{-1}, respectively. Taking into account the fact that the coefficient of isotopic shift of frequencies for D_2O is about 1.34 [12, 33], these new bands should be attributed to deformation and valent vibrations of D_2O molecules in the crystallohydrate. Table 4 shows the absorption frequencies of the bands observed and their designations.

Beside absorption bands characteristic for D_2O, spectrum 3 shows also bands characteristic for H2O. It
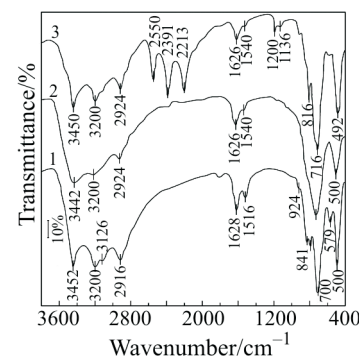

Fig. 5 Infrared absorption spectra of initial 1 – $NiSeO_3 \cdot 2H_2O$, partially dehydrated and amorphized at 2 – 473 K and after deuterated with D_2O at 3 – 473 K

means that, even at temperature of 473 K, not all H_2O molecules can be exchanged for D_2O molecules. The following two reasons were considered to explain the observation. The first one lies in the insufficient size of sample surface area leading to difficulties in the exchange for deuterium. The second one is the high activation energy of the exchange which implies strong bonds in the water molecules in $NiSeO_3 \cdot 2H_2O$. This was confirmed by the fact that full dehydration of $NiSeO_3 \cdot 2H_2O$ was achieved as high as 623 K, according to the data from the thermal analysis. It may be concluded, therefore, that both water molecules in the crystallohydrate are structurally and energetically unequal. Thus, it is impossible to obtain lower crystallohydrates ($NiSeO_3 \cdot H_2O$ and $NiSeO \cdot 1/3H_2O$) by stepwise dehydration of $NiSeO_3 \cdot 2H_2O$. They can be obtained only under conditions of hydrothermal synthesis within certain intervals of temperature and concentration of aqueous solutions of SeO_2.

Conclusions

It may be concluded, that the absorption bands observed in the IR spectra of the different selenites studied, together with the results from the powder X-ray diffraction and chemical analyses irrefutably prove the existence of different crystalline forms of nickel(II) selenites and provide enough data to determine the corresponding crystallization fields of stability in the solubility diagram of the system $NiSeO_3$–SeO_2–H_2O.

References

1 V. G. Chukhlantcev and G. P. Tomashevskii, Zh. Anal. Khim., 12 (1957) 296.
2 N. M. Selivanova, Z. L. Leshchinskaya, A. I. Maier, I. S. Streltsov and E. Yu. Muzalev, Zh. Fiz. Khim., 37 (1963) 1563.
3 Z. L. Leshchinskaya, N. M. Selivanova, A. I. Maier, I. S. Srteltsov and E. Yu. Muzilev, Zh. Vses. Obsh. D. Mendeleeva, 8 (1963) 577.
4 N. M. Selivanova and Z. L. Leshchinskaya, Zh. Neorg. Khim., 9 (1964) 259.
5 O. J. Lieder and G. Gattow, Naturwissenschaften, 54 (1967) 318.
6 O. J. Lieder and G. Gattow, Naturwissenschaften, 54 (1967) 443.
7 R. A. Muldagalieva, A. S. Pashinkin, E. A. Buketov and S. S. Bakeeva, Trudy Khim. Metalurg. Inst. Acad. Nauk Kazakh. SSR, 9 (1969) 11.
8 S. S. Bakeeva, E. A. Buketov and A. S. Pashinkin, Trudy Khim. Metalurg. Inst. Acad. Nauk Kazakh. SSR, 9 (1969) 16.
9 V. N. Makatun, R. Ya. Melnikova, V. V. Pechkovskii and L. M. Afanasev, Dokl. Akad. Nauk SSSR, Ser. Khim., 213 (1973) 353.
10 V. N. Makatun, V. V. Pechkovskii, R. Ya. Melnikova and M. N. Ryer, Russ. J. Inorg. Chem., 19 (1974) 1851.
11 K. Kohn, K. Inone, O. Horie and S. Akimoto, J. Solid State Chem., 18 (1976) 27.
12 M. Ebert, Z. Mička and I. Peková, Coll. Czech. Chem. Comm., 47 (1982) 2069.
13 M. Wildner, Monatsh. Chem., 122 (1991) 585.
14 A. V. P. McManus, W. T. A. Harrison and A. K. Cheethan, J. Solid State Chem., 92 (1991) 253.
15 K. Unterderweide, B. Engelen and K. Boldt, J. Mol. Struct., 322 (1994) 233.
16 B. Engelen, K. Boldt, K. Unterderweide and U. Baumer, Z. Anorg. Allg. Chem., 621 (1995) 331.
17 U. Baumer, K. Boldt, B. Engelen, H. Muller and K. Unterderweide, Z. Anorg. Allg. Chem., 625 (1999) 395.
18 V. P. Verma, Thermochim. Acta, 327 (1999) 63.
19 J. A. Mandarino, Eur. J. Mineral., 6 (1994) 337.
20 L. T. Vlaev, S. D. Genieva and G. G. Gospodinov, J. Therm. Anal. Cal., 81 (2005) 469.
21 A. Kotarski, Chemia Analityczna, 10 (1965) 161.
22 R. Pribil, Complexonometry (in Bulgarian), Izd. Thehnika, Sofia 1980.
23 G. G. Gospodinov and M. G. Stancheva, J. Therm. Anal. Cal., 78 (2004) 1057.
24 G. G. Gospodinov and M. G. Stancheva, J. Therm. Anal. Cal., 81 (2005) 141.
25 G. F. Pinaev and V. P. Volkova, Zh. Neorg. Khim., 21 (1976) 1341.
26 A. W. Coats and J. P. Redfern, Nature, 201 (1964) 68.
27 A. W. Coats and J. P. Redfern, J. Polym. Sci., Part B, 3 (1965) 917.
28 A. Simon and R. Paetzold, Z. Anorg. Allg. Chem., 303 (1960) 39, 46.
29 A. Simon and R. Paetzold, Z. Anorg. Allg. Chem., 303 (1960) 53.
30 C. A. Cody, R. C. Levitt, R. S. Viswanath and P. J. Miller, J. Solid State Chem., 26 (1978) 281.
31 R. S. Viswanath, P. J. Miller and C. A. Cody, J. Phys. Chem. Solids, 40 (1979) 223.
32 R. Ya. Melnikova, V. N. Makatun and V. V. Pechkovskii, Zh. Neorg. Chim., 19 (1974) 1864.
33 M. Ebert, Z. Mička and I. Pekova, Chemicke Zvesti, 36 (1982) 169.
34 G. G. Gospodinov, L. M. Sukova and K. I. Petrov, Zh. Neorg. Khim., 33 (1988) 1970; 1975.
35 V. P. Verma and A. Khushu, J. Thermal Anal., 35 (1989) 1157.
36 V. V. Pechkovskii, V. N. Makatun and R. Ya. Melnikova, Zh. Neorg. Khim., 18 (1973) 2023.
37 V. N. Makatun, R. Ya. Melnikova and T. I. Baranikova, Koord. Khim., 1 (1975) 920.
38 P. A. Giguere and M. Falk, Spectrochim. Acta, 16 (1960) 1.
39 V. V. Pechkovskii and V. N. Makatun, Zh. Neorg. Khim., 15 (1970) 2052.